Computational medical imaging: from model-based approaches to machine learning

Adrian Basarab

Université de Toulouse, IRIT, Université Paul Sabatier Toulouse 3

ICABME 2019, Tripoli, Lebanon

Outline of the talk

What is medical imaging ?

- Visualization of body parts, tissues or organs, for use in clinical diagonsis, treatment and disease monitoring

- Anatomical vs Functional

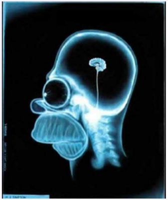

Medical imaging modalities

- Nuclear medicine (SPECT, PET)
- Radiology techniques (X-ray radiography, CT, MRI, Ultrasound)

- Scanners

Computational medical imaging

- Data inversion

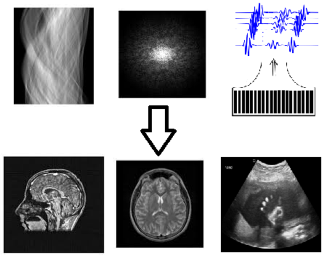

- Incomplete data, non-traditional sensing, etc.

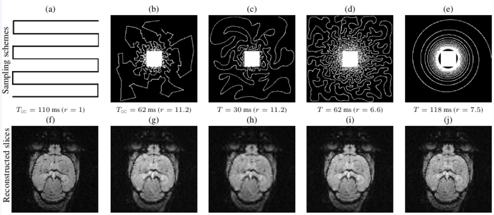

Incomplete data in ultrasound

- Computational methods to compensate for the lack of data

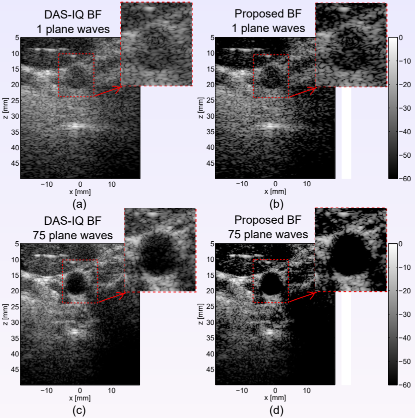

. Winner of plane-wave imaging challenge in medical ultrasound, *IEEE IUS*, 2016.

. T. Szasz, A. Basarab, D. Kouamé, Beamforming through regularized inverse problems in ultrasound medical imaging, *IEEE TUFFC*, 2016.

Outline of the talk

Inverse problems

$$\mathbf{y} = T(\mathbf{x}) + \mathbf{n}$$

- $\mathbf{y} \in \mathbb{C}^M$ is the observed data (image)
- $\mathbf{x} \in \mathbb{C}^N$ is the image of interest (not observed)
- $\mathbf{n} \in \mathbb{C}^M$ is the noise

T is the observation (forward) operator

- known : estimate $\mathbf{x}$ from $\mathbf{y}$
- unknown : estimate $\mathbf{x}$ and T from $\mathbf{y}$

Inverse problems in computational medical imaging are usually ill-posed

- T is not invertible, an infinity of solutions may exist
- A small perturbation on the data may cause an important variation on the estimate (e.g. Fourier measurements)

Solution

$$\hat{\mathbf{x}} = \arg\min_{\mathbf{x}} \|\mathbf{y} - T(\mathbf{x})\|_2^2 + \lambda r(\mathbf{x})$$

Outline of the talk

Basics on acoustic microscopy

Single-element transducer

- Very high frequency (> 50 MHz) : 250 MHz or 500 MHz
- Spherically-focused (F-number < 1.3)

Raster scan

- RF data, reflected from each scanned position, yield 3D data volume
- Acoustic parameters estimated at each position form 2D maps

Challenges

- Scanning time of 5 minutes for 1 mm by 1 mm sample
- Tissue properties may change during scanning
- Decrease the acquisition time and data amount, reduce equipment costs

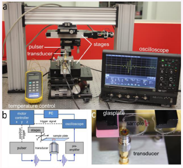

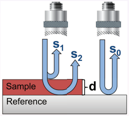

Data acquisition

Raster scan

- For each (x_1, x_2) position, RF data composed of two main reflections is digitized and saved, yielding to a 3D data volume (x_1, x_2, t)
- Speed of sound, acoustic impedance and attenuation are estimated at each scan location (x_1, x_2) to form quantitative 2D parameter maps

Example of impedance map

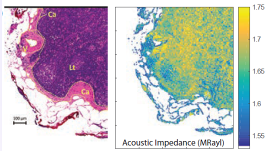

Example of speed of sound

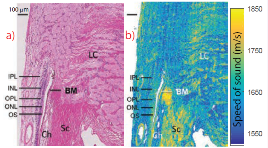

Outline of the talk

Proposed data acquisition process

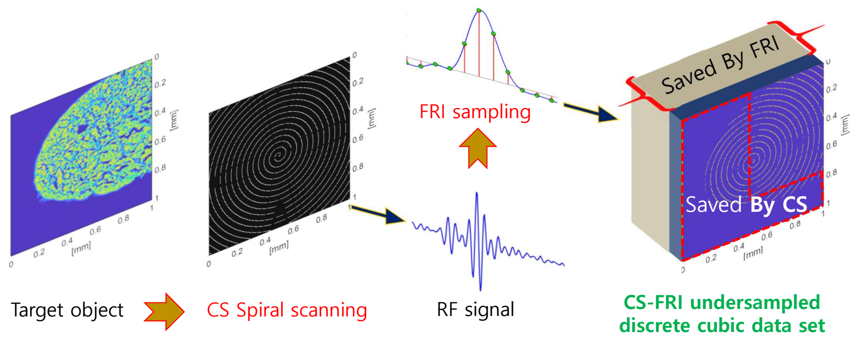

- Spiral pattern (Φ) scanning in **spatial domain**, $\boldsymbol{y} = \Phi \boldsymbol{x} + \boldsymbol{n}$
- Innovation rate ($\rho = 1/T$) sampling in **time domain**, $x_n = \left\langle \sum_{l=0}^{L-1} a_l h(t - t_l), \varphi\left(\frac{t}{T} - n\right) \right\rangle$

. J. Kim, J. Mamou, D. Kouamé, A. Achim, and A. Basarab, Spatio-temporal compressed quantitative acoustic microscopy, *IEEE IUS*, Oct 2019.

. J. Kim, J. Mamou, P. R. Hill, N. Canagarajah, D. Kouamé, A. Basarab, and A. Achim, Approximate message passing reconstruction of quantitative acoustic microscopy images, *IEEE Trans. on UFFC*, Mar 2018.

. J. Kim, J. Mamou, D. Kouamé, A. Achim, and A. Basarab, Reconstruction of quantitative acoustic microscopy images from rf signals sampled at innovation rate, *IEEE IUS*, Oct 2018.

Outline of the talk

Compressed sensing (CS)

- Sampling signals parsimoniously, acquiring only the relevant signal information, rather than sampling followed by compression
- Direct model

$$\boldsymbol{y} = \Phi \boldsymbol{x} + \boldsymbol{n}$$

  - $\boldsymbol{y} \in \mathbb{R}^M$: measurement vector
  - $\Phi \in \mathbb{R}^{M \times N}$: measurement matrix
  - $\boldsymbol{x} \in \mathbb{R}^N$: image to be reconstructed, $M << N$
  - $\boldsymbol{n} \in \mathbb{R}^M$: zero-mean additive white Gaussian noise
- Reconstruction

$$\hat{\boldsymbol{\theta}}_x = \min_{\boldsymbol{\theta}_x} \|\boldsymbol{\theta}_x\|_1 \quad \text{subject to} \quad y = \Phi W^{-1} \boldsymbol{\theta}_x$$

  - W is a sparsifying transform, $\boldsymbol{\theta}_x = W\boldsymbol{x}$

. D.L. Donoho, Compressed sensing, *IEEE Trans. on Information Theory*, 2006.

. E. Candès, J. Romberg, T. Tao, Robust Uncertainty Principles : Exact Signal Reconstruction from Highly Incomplete Fourier Information, *IEEE Trans. on Information Theory*, 2006.

Sensing pattern

- Experimental constraints
  - Point-wise acquisition
  - RF data acquired continuously as the motor stages are moved
- Proposed solution
  - Spiral sensing originating in the center of the area to be sampled
  - The pace of the spreading is used to prescribe the measurement rate
- Example of spiral pattern for a measurement rate of 20%

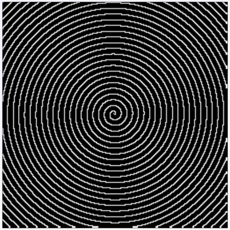

. J-H. Kim, J. Mamou, P.R. Hill, N.Canagarajah, D. Kouamé, A. Basarab, A. Achim, Approximate Message Passing Reconstruction of Quantitative Acoustic Microscopy Images, *IEEE TUFFC*, 2018.

AMP algorithm

- Iterative signal reconstruction algorithm
  - Turns the reconstruction problem into an iterative denoising approach

$$\boldsymbol{\theta}_x^{t+1} = \eta_t\left(\Theta^T \boldsymbol{z}^t + \boldsymbol{\theta}_x^t\right)$$

$$\boldsymbol{z}^t = \boldsymbol{y} - \Theta\boldsymbol{\theta}_x^t + \frac{1}{\delta}\boldsymbol{z}^{t-1}\langle\eta_{t-1}^{'}(\Theta^T\boldsymbol{z}^{t-1} + \boldsymbol{\theta}_x^{t-1}\rangle$$

  - t : iterative index
  - $\Theta = \Phi W^{-1}$
  - $\eta_t(\cdot)$, $\eta_t^{'}(\cdot)$: denoising function and its first derivative
  - δ : measurement rate M/N
  - $z^t \in \mathbb{R}^M$: current residual (error)

. D. L. Donoho, A. Maleki, A. Montanari, Message passing algorithms for compressed sensing, *Proc. Nat. Academy Sci.*, 2009.

Wavelet-based Cauchy AMP

- Assumptions
  - Wavelet coefficients provide a sparse representation for natural images
  - They can be accurately modelled using heavy tailed distributions
- Design the denoising function η
  - Based on the hypothesis of Cauchy distributed wavelet coefficients of QAM images

$$P(w) = \frac{\gamma}{w^2 + \gamma^2}$$

  - w is the wavelet coefficient
  - γ is the dispersion parameter

. A. Achim and E. E. Kuruoglu, Image denoising using bivariate α-stable distributions in the complex wavelet domain, *IEEE Signal Processing Letters*, 2005.

Cauchy-AMP algorithm

- MAP estimator
  - Observed coefficient v contaminated with additive Gaussian noise ($n = v - w$)

$$\hat{w} = arg \max_{w} Pw|v(w|v)$$

  - Using Bayes' theorem and taking the logarithm form

$$\hat{w}(v) = arg \max_{w} \left[-\frac{(v-w)^2}{2\sigma_n^2} + log\left(\frac{\gamma}{w^2+\gamma^2}\right)\right]$$

  - Cancel the first derivative w.r.t. w

$$\hat{w}^3 - v\hat{w}^2 + (\gamma^2 + 2\sigma_n^2)\hat{w} - \gamma^2 v = 0$$

  - Esimate of clean wavelet coefficient w

$$\hat{w} = \eta(v) = \frac{v}{3} + s + t$$

$$\hat{w}' = \eta'(v) = 1/3 + s' + t'$$

    - s and t depend on v and σ_n^2

Cauchy-AMP algorithm

- The comparison of behaviour among four different denoisers
  - Cauchy-based
  - Soft thresholding (ST)
  - Amplitude scale invariant Bayes estimator (ABE)

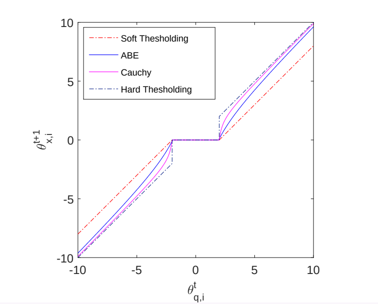

. D.L. Donoho, De-noising by soft-thresholding, *IEEE Trans. on Information Theory*, 1995.

. M. A. Figueiredo and R. D. Nowak, Wavelet-based image estimation : an empirical Bayes approach using Jeffreys' noninformative prior, IEEE Trans. on Image Processing, 2001.

Results at 30% measurement ratio

- Human lymph node

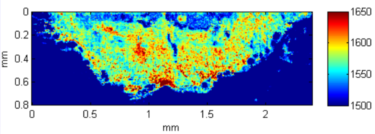

(a) Original

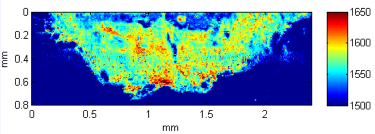

(b) AMP-Cauchy

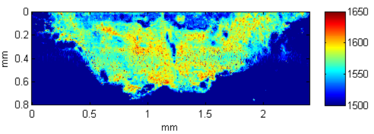

(c) AMP-ST

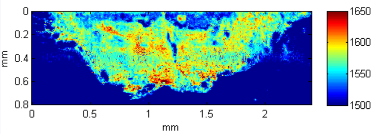

(d) AMP-ABE

- Quantitative results

Method	SSIM	PSNR
AMP-Cauchy	0.714	40.42
AMP-ST	0.683	39.98
AMP-ABE	0.708	40.10

Proposed data acquisition process

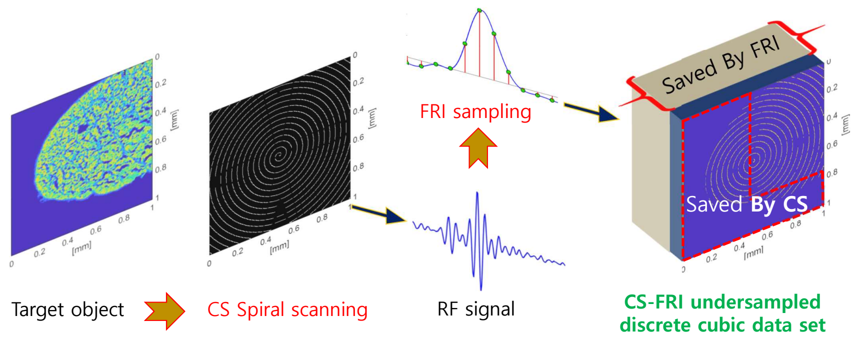

- Spiral pattern (Φ) scanning in **spatial domain**, $\boldsymbol{y} = \Phi \boldsymbol{x} + \boldsymbol{n}$
- Innovation rate ($\rho = 1/T$) sampling in **time domain**, $x_n = \left\langle \sum_{l=0}^{L-1} a_l h(t - t_l), \varphi\left(\frac{t}{T} - n\right) \right\rangle$

. J. Kim, J. Mamou, D. Kouamé, A. Achim, and A. Basarab, Spatio-temporal compressed quantitative acoustic microscopy, *IEEE IUS*, Oct 2019.

. J. Kim, J. Mamou, P. R. Hill, N. Canagarajah, D. Kouamé, A. Basarab, and A. Achim, Approximate message passing reconstruction of quantitative acoustic microscopy images, *IEEE Trans. on UFFC*, Mar 2018.

. J. Kim, J. Mamou, D. Kouamé, A. Achim, and A. Basarab, Reconstruction of quantitative acoustic microscopy images from rf signals sampled at innovation rate, *IEEE IUS*, Oct 2018.

Outline of the talk

Finite rate of innovation (FRI)

- A typical FRI signal described by a limited number of parameters

$$x(t) = \sum_{l=0}^{L-1} a_l h(t - t_l)$$

Unknown :

- t_l : time delays
- a_l : amplitude decays

Known :

- $h(t)$: pulse shape

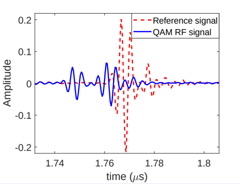

- FRI sampling by kernel $\varphi(t)$ and innovation rate ($\rho = 1/T$)

$$x_n = \left\langle \sum_{l=0}^{L-1} a_l h(t - t_l), \varphi\left(t/T - n\right) \right\rangle$$

  - ρ : total number of the unknown parameters (t_l, a_l)
- FRI recovery techniques for estimating t_l and a_l
  - Annihilating filter, matrix pencil method, etc.

. M. Vetterli, P. Marziliano, and T. Blu, Sampling signals with finite rate of innovation, *IEEE Trans. on Signal Proc.*, Jun 2002.

Acoustic parameter estimation by AR estimator

- Retrieve Fourier coefficients $X[k]$ from $x[n]$ and $\Phi(\omega)$

$$x[n] = \langle x(t), \varphi(t - nT) \rangle = \sum_{k \in Z} X[k] e^{\frac{j2\pi knT}{\tau}} \Phi^* \left[\frac{2\pi k}{\tau} \right]$$

  - $\Phi^*(\omega)$: transpose of Fourier transform of $\varphi(t)$
- The power series form acquired from $N[k] = X[k]/H[k]$

$$N[k] = \sum_{l=0}^{L-1} a_l \{\exp[\Delta f(\beta_l + j2\pi t_l)]\}^k = \sum_{l=0}^{L-1} a_l \lambda_l^k$$

- AR model construction

$$N_k = \sum_{i=1}^{n} s_i N_{k-i} + \epsilon_k$$

- Calculation of acoustic parameters from identified λ_l and a_l

---

. J-H. Kim, J. Mamou, D. Kouamé, A. Achim, A. Basarab, Autoregressive model-based reconstruction of quantitative acoustic maps from RF signals sampled at innovation rate, submitted to *IEEE TCI*, 2019.

. D. Rohrbach and J. Mamou, Autoregressive signal processing applied to high-frequency acoustic microscopy of soft tissues, *IEEE Trans. on UFFC*, 2018.

Outline of the talk

Illustration of the images at each reconstruction stage

- Speed of sound (SOS) maps of chicken tendon acquired with a 250 MHz transducer

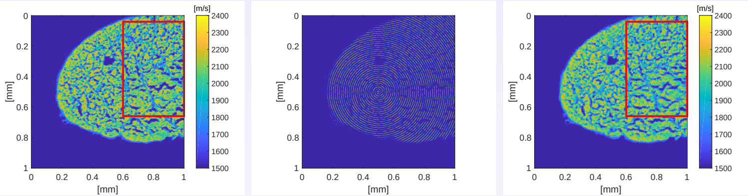

(a) (b) (c)

- (a) : Conventional sampling at $1\mu m$ by $1\mu m$
- (b) : The spiral masking area recovered by FRI framework
- (c) : FRI-CS recovery

Comparison of reconstructed images

- Chicken tendon 2D SOS maps

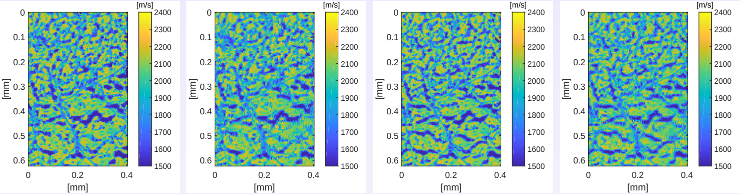

(a) Conventional approach (b) CS recovery (c) FRI recovery (d) FRI-CS recovery

- Quantitative results

Methods	PSNR(dB)	NRMSE	SSIM	compressed ratio (%)	Acquisition times
CS (b)	26.31	0.0483	0.7166	40	5%
FRI (c)	24.19	0.0617	0.6741	6.5	100%
FRI-CS (d)	23.38	0.0678	0.5511	2.6	5%

Outline of the talk

Super-resolution

- Tensor-based super-resolved 3D CBCT

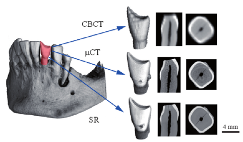

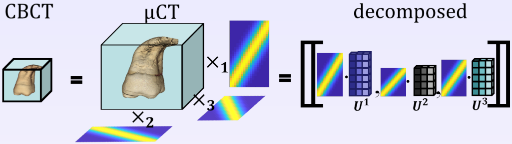

- MR-ultrasound image fusion

MRI

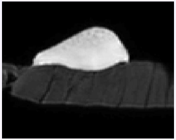

Ultrasound

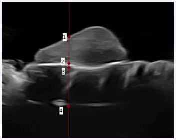

Fusion

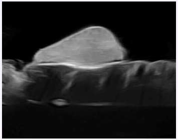

. J. Hatvani, A. Basarab, J.-Y. Tourneret, M. Gyongy, D. Kouamé, A Tensor Factorization Method for 3D Super-Resolution with Application to Dental CT, *IEEE TMI*, 2019.

. O. El Mansouri, A. Basarab, F. Vidal, D. Kouamé, J.-Y. Tourneret, Fusion of Magnetic Resonance and Ultrasound Images : a Preliminar Study on Simulated Data, *IEEE ISBI*, 2019.

Cardiac motion estimation

Let $\boldsymbol{I}_k \in \mathbb{R}^N$, $\boldsymbol{I}_{k+1} \in \mathbb{R}^N$ be two consecutive images

- The motion field to be estimated is $\boldsymbol{U_k} = (\boldsymbol{u_k}^T, \boldsymbol{v_k}^T)^T \in \mathbb{R}^{2N}$

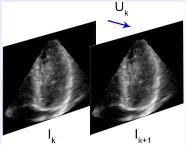

Minimization of an energy function

$$\min_{\alpha, \boldsymbol{U}} \{E_{\text{data}}(\boldsymbol{U}, \boldsymbol{I}) + \lambda_s E_{\text{spatial}}(\boldsymbol{U}) + \lambda_d E_{\text{sparse}}(\boldsymbol{U}, \boldsymbol{D}, \alpha)\}$$

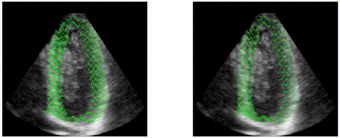

. N. Ouzir, A. Basarab, O. Lairez, and J.-Y. Tourneret, Robust Optical Flow Estimation in Cardiac Ultrasound images Using a Sparse Representation, *IEEE TMI*, 2018.

. N. Ouzir, A. Basarab, H. Liebgott, B. Harbaoui, and J.-Y. Tourneret, Motion estimation in echocardiography using sparse representation and dictionary learning, *IEEE TIP*, 2018.

Outline of the talk

Spatial resolution in acoustic microscopy

Dependent on the central frequency

- Increasing the frequency comes with
  - Increased costs associated with the transducer and the necessary electronics
  - Experimental difficulties (e.g., sensitivity to nm scale vibrations and temperature)

Example of impedance images on a section of cancerous human lymph node

- Thin section of soft tissue (12 μm) affixed to a microscopy slide

250 MHz

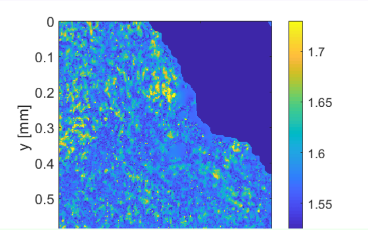

500 MHz

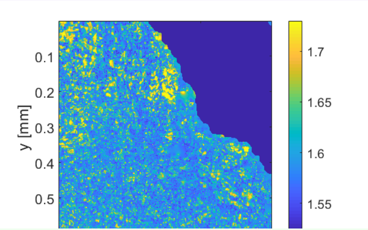

Outline of the talk

Forward model

$$\mathbf{y} = \mathbf{SHx} + \mathbf{n}$$

- $\mathbf{y} \in \mathbb{R}^{N_l \times 1}$: is the measured image, $N_l = m_l \times n_l$
- $\mathbf{x} \in \mathbb{R}^{N_h \times 1}$: super-resolved image to be estimated, $N_h = d^2 N_l$
- $\mathbf{n} \in \mathbb{R}^{N_l \times 1}$: Gaussian noise

Degradation operators

- $\mathbf{H} \in \mathbb{R}^{N_h \times N_h}$: 2D circulant convolution matrix (PSF of the transducer)
- $\mathbf{S} \in \mathbb{R}^{N_l \times N_h}$: subsampling operator

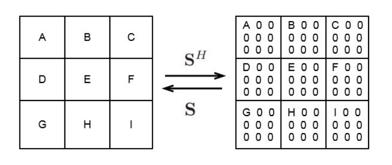

SR optimization problem

- Super-resolved slice $\mathbf{x}_t$ estimation (time subscript is omitted in the following)

$$\min_{\mathbf{x}} \frac{1}{2}\|\mathbf{y} - \mathbf{SHx}\|_2^2 + \tau\phi(\mathbf{Ax})$$

- Total variation regularization

$$\phi(\mathbf{Ax}) = \sqrt{\|\mathbf{D}_\mathrm{h}\mathbf{x}\|^2 + \|\mathbf{D}_\mathrm{v}\mathbf{x}\|^2}$$

$\mathbf{A} = [\mathbf{D}_\mathrm{h}, \mathbf{D}_\mathrm{v}]^T \in \mathbb{R}^{2N_h \times N_h}$

- Constrained optimization

$$\begin{aligned} \min_{\mathbf{x},\mathbf{u}} \quad & \frac{1}{2}\|\mathbf{y} - \mathbf{SHx}\|_2^2 + \tau\phi(\mathbf{u}) \\ \text{subject to} \quad & \mathbf{Ax} = \mathbf{u} \end{aligned}$$

- Associated augmented Lagrangian function

$$\mathcal{L}(\mathbf{x}, \mathbf{u}, \lambda) = \frac{1}{2}\|\mathbf{y} - \mathbf{SHx}\|_2^2 + \tau\phi(\mathbf{u}) + \frac{\mu}{2}\|\mathbf{Ax} - \mathbf{u} + \lambda\|_2^2$$

ADMM-based algorithm

Iterate

$\mathbf{x}^{k+1} = \arg\min_{\mathbf{x}} \|\mathbf{y} - \mathbf{SHx}\|_2^2 + \mu\|\mathbf{Ax} - \mathbf{u}^k + \mathbf{d}^k\|_2^2$

$\mathbf{u}^{k+1} = \arg\min_{\mathbf{u}} \tau\phi(\mathbf{u}) + \frac{\mu}{2}\|\mathbf{Ax}^{k+1} - \mathbf{u} + \mathbf{d}^k\|_2^2$

$\mathbf{d}^{k+1} = \mathbf{d}^k + (\mathbf{Ax}^{k+1} - \mathbf{u}^{k+1})$

until stopping criterion is satisfied.

Update **u** *using the vector-soft-thresholding operator*

$$\begin{aligned} \boldsymbol{\nu} &= [\mathbf{D}_{\mathrm{h}}\mathbf{x}^{k+1} + \mathbf{d}_{\mathrm{h}}^k, \mathbf{D}_{\mathrm{v}}\mathbf{x}^{k+1} + \mathbf{d}_{\mathrm{v}}^k] \\ \mathbf{u}^{k+1}[i] &= \max\{\mathbf{0}, \|\boldsymbol{\nu}[i]\|_2 - \tau/\mu\}\frac{\boldsymbol{\nu}[i]}{\|\boldsymbol{\nu}[i]\|_2} \end{aligned}$$

Update **x** *using a closed-form solution exploiting the following property of* **S**

$$\mathbf{FS}^H\mathbf{SF}^H = \frac{1}{d}\mathbf{J}_d \cdot \mathbf{I}_{N_l}$$

. N. Zhao, Q. Wei, A. Basarab, N. Dobigeon, D. Kouamé, J.-Y. Tourneret, Fast Single Image Super-resolution using a New Analytical Solution for ℓ_2-ℓ_2 Problems, *IEEE TIP*, 2016.

Resolution target results

USAF 1951 resolution phantom

- Super-resolution factor $d = 2$

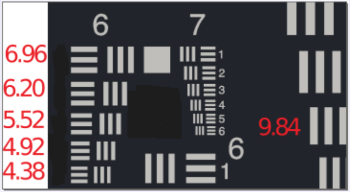

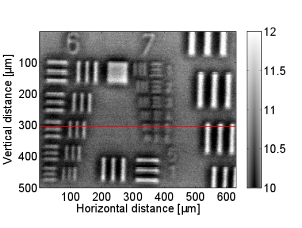

Horizontal profiles

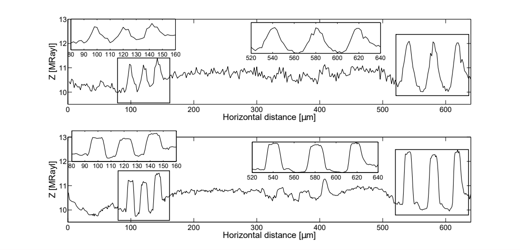

Model-based super-resolution

Fails on ex vivo samples

- Convolution with the PSF not sufficient to model the 250 MHz images

Example of impedance images on a section of cancerous human lymph node

- Thin section of soft tissue (12 μm) affixed to a microscopy slide

500 MHz | 250 MHz | Enhanced 250 MHz

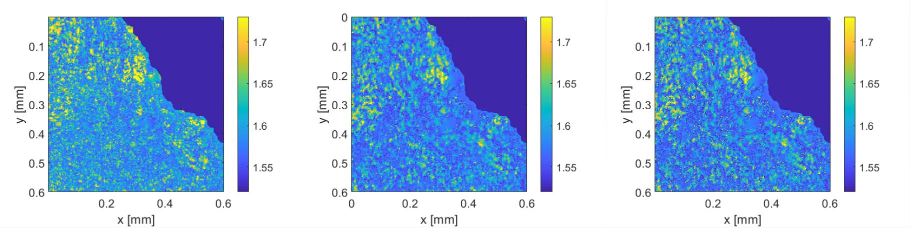

Outline of the talk

Data-driven super-resolution

Fully convolution neural network (U-net) trained on 250 and 500 MHz images

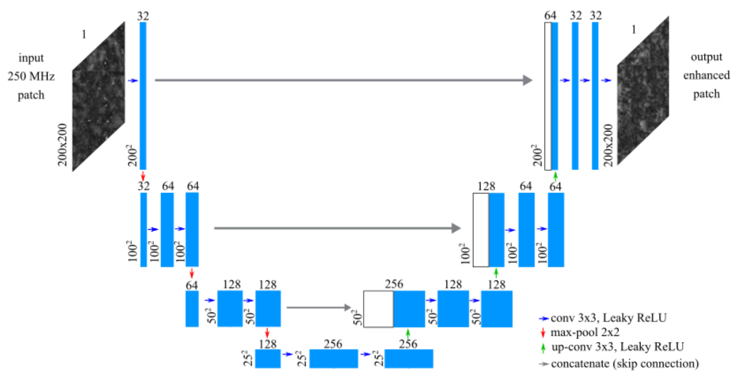

. J. Mamou, T. Pellegrini, D. Kouamé, A. Basarab, A convolutional neural network for 250-MHz quantitative acoustic-microscopy resolution enhancement , *IEEE EMBC*, 2019.

Results

500 MHz 250 MHz Enhanced 250 MHz

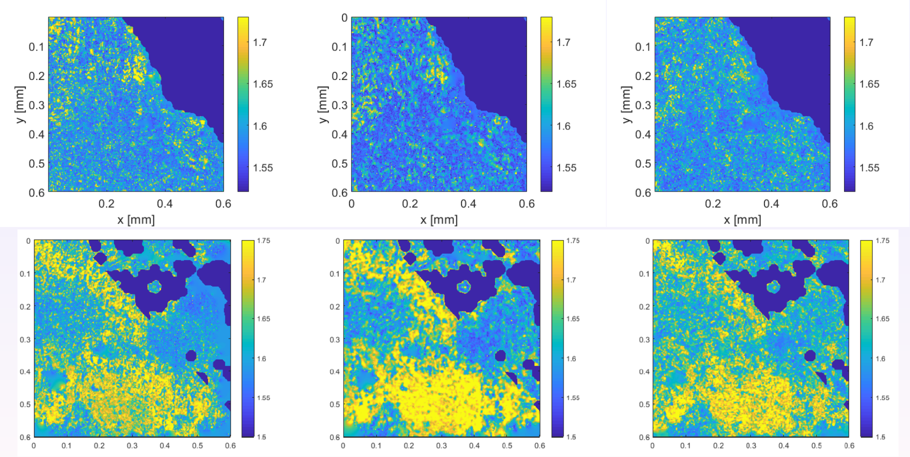

Conclusions

Computational imaging

- In most of medical applications data is not sufficient to form the image (noise, incomplete data)
- Computational methods are used to avoid the ill-posedness of the resulting inverse problem

Model-based approaches

- Models include knowledge about the physics : fidelity, tractability ?
- Regularization terms are required and usually use adaptive or non-adaptive transforms : appropriate choice ?

Data-driven approaches

- More flexibility, but usually require learning databases
- How to include knowledge about the physics ?
- Forward model, regularization, both ?

Computational medical imaging: from model-based approaches to machine learning

Adrian Basarab

Université de Toulouse, IRIT, Université Paul Sabatier Toulouse 3

ICABME 2019, Tripoli, Lebanon